

# Selectivity of photocatalytic oxidation of gaseous ethanol over pure and modified TiO<sub>2</sub>

Alexandre V. Vorontsov\* and Vera P. Dubovitskaya

*Boriskov Institute of Catalysis, Novosibirsk 630090, Russia*

Received 30 April 2003; revised 22 August 2003; accepted 5 September 2003

## Abstract

The rates of the two main stages of photocatalytic ethanol destruction—oxidation of ethanol to acetaldehyde and oxidation of acetaldehyde to CO<sub>2</sub>—were studied under varied concentrations of ethanol and acetaldehyde and photocatalyst irradiance, at different temperatures, and over different photocatalysts. The rates followed the semiempirical three sites Langmuir–Hinshelwood model that envisages sites for ethanol and acetaldehyde adsorption and additional sites for competitive adsorption of ethanol and acetaldehyde. The increase in irradiance gave rise to higher selectivity toward CO<sub>2</sub> via increased concentrations of gaseous intermediate acetaldehyde. However, the rate of ethanol oxidation rose faster than the rate of acetaldehyde oxidation. The selectivity toward CO<sub>2</sub> monotonically decreased with temperature over TiO<sub>2</sub> and the rate of oxidation reached a maximum at 80 °C. Among platinum-doped catalysts, the best activity was found for 1.1% Pt/TiO<sub>2</sub>. Platinum addition to TiO<sub>2</sub> resulted in a 1.5- to 2-fold increased overall rate of oxidation. The selectivity to CO<sub>2</sub> over Pt/TiO<sub>2</sub> catalyst monotonically increased with temperature. Separate studies in a batch reactor demonstrated that addition of platinum changed the product distribution. Acetic acid, instead of carbon monoxide, was formed in copious quantities over the Pt/TiO<sub>2</sub> catalyst.

© 2003 Elsevier Inc. All rights reserved.

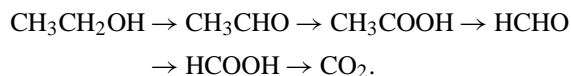
**Keywords:** Photocatalysis; Langmuir–Hinshelwood; Temperature; Platinization; Irradiance; Light intensity; Photocatalytic activity

## 1. Introduction

Photocatalytic oxidation was proposed as an advantageous method of air purification from organic pollutants. One of the problems preventing its immediate practical application is the possibility of releasing dangerous intermediate products during air purification. Ethanol and other alcohols are relatively innocuous air pollutants. Ethanol is commonly used as a solvent. Removal of its vapors from air is also important for bakeries and breweries. Photocatalytic oxidation is a very interesting method for treatment of air with a low concentration of pollutants. However, many researchers have demonstrated that acetaldehyde, a more toxic compound, is formed as a by-product in photocatalytic oxidation of ethanol [1–11]. Additional research is necessary to minimize production of aldehydes in photocatalytic purification.

The kinetics and mechanism of ethanol photocatalytic oxidation over TiO<sub>2</sub> have been studied extensively previously.

Nimlos et al. detected acetaldehyde, acetic acid, formaldehyde, and formic acid as intermediate products in gaseous ethanol photocatalytic oxidation in a batch reactor [2]. They suggested the following reaction scheme:



Acetaldehyde is the main gaseous intermediate, and the concentration of other products in the gas phase is usually much lower. The main reaction scheme shown above is sometimes accompanied by several other intermediates in low concentrations such as methyl formate, ethyl formate, methyl acetate [2], and 1,1-diethoxyethane [10]. These products obviously result from condensation reactions between the main intermediate products. Carbon dioxide and water are invariably the final products of the oxidation over TiO<sub>2</sub>.

Muggli and co-workers [3,5,6,8] used low-contact-time flow reactor and temperature-programmed techniques to study ethanol photocatalytic oxidation. Using  $\alpha$ -<sup>13</sup>C-labeled ethanol they found that the  $\alpha$ -carbon is oxidized into CO<sub>2</sub> faster than the  $\beta$ -carbon. Acetaldehyde was the gaseous intermediate of ethanol oxidation only if high initial surface

\* Corresponding author.

E-mail address: [voronts@catalysis.nsk.su](mailto:voronts@catalysis.nsk.su) (A.V. Vorontsov).

coverages of ethanol were used. They detected acetaldehyde, acetic acid, formaldehyde, and formic acid on the  $\text{TiO}_2$  surface after ethanol photocatalytic oxidation. Two types of ethanol adsorption sites with weak and strong adsorption were found. Acetaldehyde desorbs as an intermediate product only from the site with weak ethanol adsorption. Poisoning of the sites with strong adsorption by acetaldehyde generated a photocatalyst with high selectivity for acetaldehyde production. This result can be useful for synthesis of acetaldehyde. For air purification, one would prefer photocatalyst with low selectivity for acetaldehyde. Acetaldehyde is thought to react differently on two different  $\text{TiO}_2$  sites—with and without forming acetic acid.

Kozlov et al. studied [11] ethanol photocatalytic oxidation using FTIR. They detected surface acetic acid, acetaldehyde, carboxylates, and carbonate as intermediate products, generally confirming the results obtained by other techniques.

Acetaldehyde was detected as a gaseous intermediate in the photocatalytic oxidation of ethanol and diethyl ether in a batch system [4]. The concentration of gaseous ethanol significantly changed the selectivity of oxidation. An increase of ethanol concentration from 30 to 600 ppm resulted in more than a triple decrease of the  $\text{CO}_2$  generation rate and an increase of acetaldehyde generation rate due to adsorption competition between ethanol and acetaldehyde.

Rafty co-workers [9,10] studied gas-phase ethanol photocatalytic oxidation using NMR with magic-angle spinning. They identified the two types of adsorbed ethanol—a hydrogen-bonded ethanol and titanium-bonded ethoxide. The latter species has several adsorption sites. Acetic acid was detected as an intermediate and shown to accumulate on the nonirradiated surface of  $\text{TiO}_2$ .

A complete kinetic description of the reaction network for ethanol photocatalytic oxidation in batch reactors was attempted by Sauer and Ollis [1] and Nimlos et al. [2]. Adsorption can change concentration profiles in a batch reactor [1,12] and was taken into account in [1] but complicated the description. Despite the complexity of models and large number of kinetic parameters obtained from fitting (e.g., 7 in Ref. [1]), there was significant deviation of the models from experimental data.

In the current investigation, we use a flow system with good stirring that avoids adsorption complications and which produces reliable data. Since the complete kinetic model of ethanol photocatalytic oxidation is rather complex, we developed a semiempirical model for the dependence of ethanol and acetaldehyde oxidation rates on conditions that take into account two types of adsorption sites. Other intermediates were not taken into account because their concentration was much lower.

In an attempt to develop a better photocatalyst for ethanol oxidation, surface modification of  $\text{TiO}_2$  with platinum was applied.

Kennedy and Datye [13] showed that platinum-doped  $\text{TiO}_2$  had a significantly increased activity in photooxida-

tion of ethanol in comparison to pure  $\text{TiO}_2$  over a wide temperature range. However, it is difficult to compare the selectivities of different catalysts used in their study because the conversions were very different over different catalysts.

We provide selectivity plots at fixed concentrations of ethanol in the reactor. We also provide comparison of reaction intermediates for platinum-doped and pure  $\text{TiO}_2$  in ethanol oxidation in a batch reactor.

## 2. Experimental

Two kinds of titanium dioxide were used in this study.  $\text{TiO}_2$  Hombifine N was supplied by Sachtleben Chemie GmbH. The BET surface area of this sample was  $347 \text{ m}^2/\text{g}$ , and it was 100% anatase. Homemade  $\text{TiO}_2$  [14] was prepared by aqueous hydrolysis of chemically pure  $\text{TiCl}_4$  and precipitation with  $\text{NaOH}$ . The deposit formed was washed thoroughly with distilled water and calcined in air at  $400^\circ\text{C}$  for 3 h. This  $\text{TiO}_2$  is 100% anatase with specific surface area  $120 \text{ m}^2/\text{g}$ . Both photocatalysts demonstrated similar activity in acetone photocatalytic oxidation. The samples were loaded with Pt using reduction with  $\text{NaBH}_4$  as detailed below.  $\text{TiO}_2$  was impregnated with an aqueous solution of  $\text{H}_2\text{PtCl}_6$  followed by dropwise addition of a threefold stoichiometric quantity of cold 0.1 M  $\text{NaBH}_4$  solution under rapid stirring. Before drying at  $60^\circ\text{C}$ , the resultant Pt/ $\text{TiO}_2$  samples were washed with distilled water and centrifuged 10 times. The platinum content was ascertained by X-ray fluorescence analysis using a VRA-20 instrument with a W anode and did not deviate significantly from the content aimed for.

Photocatalytic reactions were performed in batch and flow-circulating reactors. Oxygen of purified air was the oxidant in both reactors. The batch reactor was a  $449 \text{ cm}^3$  glass vessel with a quartz window. A magnetic stirrer was used to stir the air inside the reactor. Twenty milligrams of each photocatalyst was deposited onto a glass plate and placed into the reactor. Then  $2 \mu\text{l}$  of ethanol was injected in the reactor. Illumination began after complete evaporation of ethanol.

The flow-circulating system was described in detail previously [4]. The main feature of this system is that it provided a uniform concentration of reactants and products inside the system, which allowed reliable kinetic measurements. Samples of catalysts were deposited onto glass plates from aqueous suspension to form nontransparent film with geometric area  $3.1 \text{ cm}^2$ .

Reactants and products were analyzed using gas chromatographs equipped with FID and TCD. Carbon dioxide was determined on a FID after converting it into methane by catalytic reaction with hydrogen.

A LOS-2 illuminator equipped with a 1000 W Xe lamp was employed in this study. The intensity of UV light was varied by changing the size of an aperture in the illuminator and inserting/removing a 313-nm interference filter.

The rate of acetone oxidation was calculated from the rate of  $\text{CO}_2$  generation, and  $\text{CO}_2$  was the only significant carbonaceous gaseous product of oxidation. The carbon mass balance calculated from acetone and  $\text{CO}_2$  concentrations was closed within 10% for all experiments on acetone photocatalytic oxidation. Since acetaldehyde was an important gaseous intermediate of ethanol oxidation, it was more difficult to give adequate activity of catalysts in ethanol oxidation. This issue is considered in the next section.

### 3. Results and discussion

Photocatalytic oxidation of ethanol was demonstrated to be a two-step process with acetaldehyde as the main gaseous intermediate, e.g. [4]:



Throughout this paper, the rate of the first reaction is designated as  $R_1$  and that of the second reaction as  $R_2$ . The selectivity of ethanol photocatalytic oxidation to  $\text{CO}_2$  is conveniently expressed as  $S = R_2/R_1$  that upon expansion coincides with the standard definition of selectivity. Throughout this paper, the carbon mass balance at steady state calculated from ethanol, acetaldehyde, and  $\text{CO}_2$  concentrations was closed within 15%. This closure is within the errors of chromatographic analysis and testifies to the absence of important gaseous intermediates besides acetaldehyde.

Since  $R_1$ ,  $R_2$ , and  $S$  are dependent on such reaction conditions as feed flow rate, the catalytic activity cannot be expressed by any of these single parameters adequately. The overall catalytic activity can be, however, expressed by the rate of consumption of oxygen  $R_0$ ,  $R_0 = R_1 + 5R_2$ . This equation is applied throughout the paper to calculate reported  $R_0$  and quantum efficiency of ethanol oxidation at different irradiance. Direct measurement of oxygen consumption rate was not possible because oxygen concentration underwent very small change as a result of oxidation.

The concentration of ethanol and acetaldehyde is expected to exert a big influence on rates of ethanol and acetaldehyde transformation in ethanol photocatalytic oxidation because of competitive adsorption. Fig. 1 demonstrates how concentrations of acetaldehyde influences  $R_1$ ,  $R_2$ , and  $R_0$  at three fixed concentrations of ethanol, 250 (Fig. 1a), 500 (Fig. 1b), and 1000 ppm (Fig. 1c). The flow-circulating reactor and  $\text{TiO}_2$  Hombifine N were used to obtain the data. The ethanol concentration in the reactor for each of the figures was kept constant using adjustments of feed ethanol concentration. The acetaldehyde concentration was changed by changing the flow rate through the reactor. The concentration of acetaldehyde was varied in approximately the same range of 200 to 900 ppm. Reaching steady state at each set of parameters took about 2 h. As we can see in Fig. 1, the increase of acetaldehyde concentration at each constant ethanol concentration resulted in an increase of acetaldehyde oxidation rate ( $R_2$ ) and a decrease of ethanol oxidation

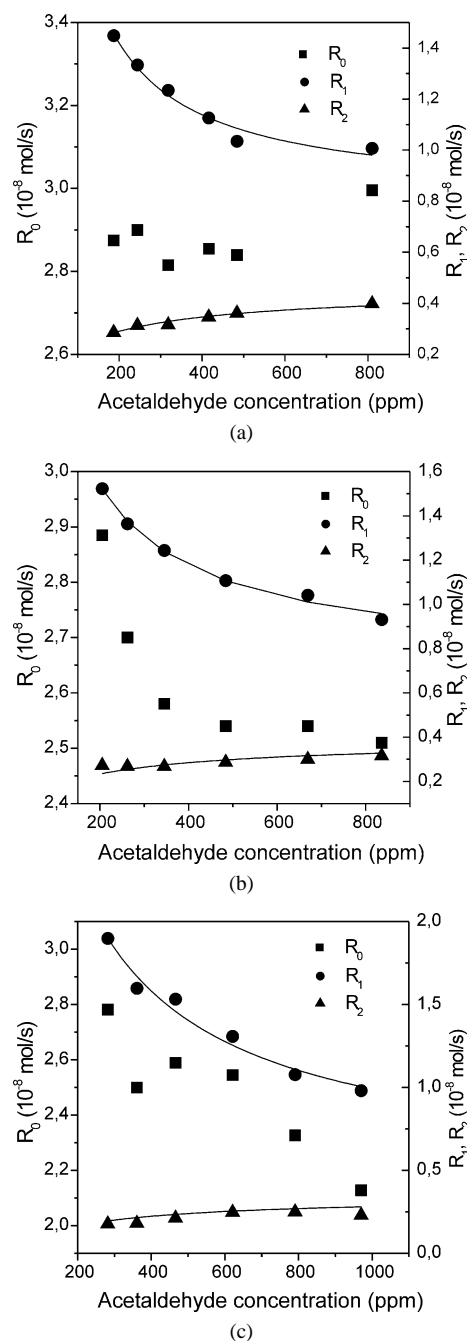


Fig. 1. Rate of ethanol  $R_1$  and acetaldehyde  $R_2$  oxidation and oxygen consumption  $R_0$  as a function of acetaldehyde concentration at different concentrations of ethanol: (a) 250 ppm, (b) 500 ppm, (c) 1000 ppm. Temperature 40 °C, water vapor concentration about 5000 ppm, Hombifine N photocatalyst mass 20 mg.

rate ( $R_1$ ). This behavior could be expected from competitive adsorption of ethanol and acetaldehyde. The oxygen consumption rate changes differently at low and high ethanol concentrations. At an ethanol concentration of 250 ppm,  $R_0$  does not change significantly with the increase in acetaldehyde concentration. The big scattering of  $R_0$  points in Fig. 1 should be attributed to the method of its calculation: the error of measuring  $R_2$  is multiplied by 5 and added to the

error of measuring  $R_1$ . At ethanol concentrations of 500 and 1000 ppm,  $R_0$  shows a marked average decrease with the growth of acetaldehyde concentration. It should be noted that  $R_0$  is similar at low concentrations of acetaldehyde at all three concentrations of ethanol. The ethanol oxidation rate  $R_1$  changes little with increasing ethanol concentration from 250 to 500 ppm, but increases markedly at an ethanol concentration of 1000 ppm. Comparing Figs. 1a, b, and c, one can see that the acetaldehyde oxidation rate  $R_2$  constantly decreases with the increase of ethanol concentration.

In the simplest case, the curves in Fig. 1 could be described by the one site Langmuir–Hinshelwood model with competitive adsorption of ethanol and acetaldehyde.

$$R_1 = \frac{k_E K_E C_E}{1 + K_E C_E + K_A C_A}, \quad R_2 = \frac{k_A K_A C_A}{1 + K_E C_E + K_A C_A}. \quad (1)$$

In Eq. (1),  $k_E$  and  $k_A$  are rate constants for ethanol and acetaldehyde,  $K_E$  and  $K_A$  are adsorption constants for ethanol and acetaldehyde, and  $C_E$  and  $C_A$  are concentration of ethanol and acetaldehyde. Water adsorption also takes part in competition. Its concentration over the catalyst changes, as a result of oxidation, within the range of 5100–6500 ppm. This change is small compared to the quadruple change of ethanol and acetaldehyde concentration. Therefore, water vapor concentration and catalyst coverage with water can be assumed constant. In this case, water vapor adsorption can be incorporated into adsorption constants of ethanol and acetaldehyde using the method reported elsewhere [12]. Oxygen takes part in oxidation as reactant and can also compete for adsorption sites. Air was used as oxygen source in this study. Oxygen concentration does not change as a result of oxidation since its concentration greatly exceeds the concentration of ethanol and acetaldehyde. Hence, its influence is included as constant factors in rate constants and adsorption constants.

Eq. (1) was used to fit the experimental data in Fig. 1 but it failed to describe the curves of  $R_1$  and  $R_2$  satisfactorily if the adsorption constants are kept constant. As we considered in the Introduction, there are two types of sites for adsorption of ethanol and acetaldehyde. Muggli and Falconer [6] measured adsorption of ethanol and acetaldehyde and found that there are sites available only for acetaldehyde, sites available for both acetaldehyde and ethanol, and some sites available only for ethanol. Following these results, we used three types of adsorption sites for the ethanol oxidation model. The following equations describe the three-site photocatalytic oxidation of ethanol and acetaldehyde:

$$R_1 = R_E + \frac{k_E K_E C_E}{1 + K_E C_E + K_A C_A}, \quad (2)$$

$$R_2 = \frac{k_A^A K_A^A C_A}{1 + K_A^A C_A} + \frac{k_A K_A C_A}{1 + K_E C_E + K_A C_A}. \quad (3)$$

In Eq. (2),  $R_E$  represents the rate of ethanol photocatalytic oxidation on sites not available for acetaldehyde,  $k_E$  and  $K_E$  are rate and adsorption constants of ethanol and  $K_A$  is acetaldehyde adsorption constant on sites available for both acetaldehyde and ethanol. In Eq. (3), the first part represents the rate of acetaldehyde oxidation on sites not available for ethanol:  $k_A^A$  and  $K_A^A$  are rate and adsorption constants of acetaldehyde on these sites. The reason why  $R_E$  in Eq. (2) was not expanded as in Eq. (3) will be explained below.

Eqs. (2) and (3) were fitted to the experimental data in Fig. 1 and the curves in Fig. 1 represent the fit results. Table 1 lists the kinetic parameters obtained in the fitting procedure. Contrary to expectations, the rate of ethanol oxidation  $R_E$  on sites not available for acetaldehyde decreases with the increase of ethanol oxidation. The model does not take into account concentrations of surface intermediate products other than acetaldehyde. However, they can also compete for the same sites with ethanol. A higher concentration of ethanol is expected to give a higher concentration of acetic acid as observed previously in a study by Muggli et al. [8]. Therefore, the decrease of  $R_E$  is attributable to competition of ethanol with surface intermediate products.

Light intensity, or irradiance, is among the easily changeable conditions of photocatalytic oxidation. Changing the irradiance can improve the conversion of ethanol into the products of its complete destruction and changes the reaction selectivity. We changed the irradiance from about 0.5 to  $14 \times 10^{-8}$  E/(s cm<sup>2</sup>). Fig. 2 represents the effect of irradiance on ethanol photocatalytic oxidation under constant concentration of ethanol at 300 ppm, which was obtained in the flow-circulating reactor over Hombifine N photocatalyst. One can see that the increase in irradiance results in an increase of ethanol ( $R_1$ ) and acetaldehyde ( $R_2$ ) oxidation rates, an increase of selectivity to CO<sub>2</sub>, an increase of oxygen consumption rate, and a decrease of the quantum efficiency of oxygen consumption. The increase in irradiance increases the rates of the photocatalytic reactions and this leads to the increase of the acetaldehyde concentration in the reactor from 71 ppm for the lowest irradiance to 583 ppm for the highest irradiance in Fig. 2. It would be very difficult to keep concentrations of both ethanol and acetaldehyde constant in the reactor. This increase in acetaldehyde concentration explains, at least partially, the increase of selectivity to CO<sub>2</sub> with the increase of irradiance. If we assume that the adsorption constants are irradiance independent, which is a usual assumption in photocatalysis, then irradiance should

Table 1  
Kinetic parameters obtained from fitting Eqs. (2) and (3) to data in Fig. 1

$R_E$ ( $10^{-8}$ mol/s)	$k_E$ ( $10^{-8}$ mol/s)	$K_E$ (ppm <sup>-1</sup> )	$K_A$ (ppm <sup>-1</sup> )	$k_A^A$ ( $10^{-8}$ mol/s)	$K_A^A$ (ppm <sup>-1</sup> )	$k_A$ ( $10^{-8}$ mol/s)
0.81 ( $C_E$ 250 ppm)						
0.74 ( $C_E$ 500 ppm)	4.5	0.08	0.1	0.004	0.25	0.1
0.47 ( $C_E$ 1000 ppm)						

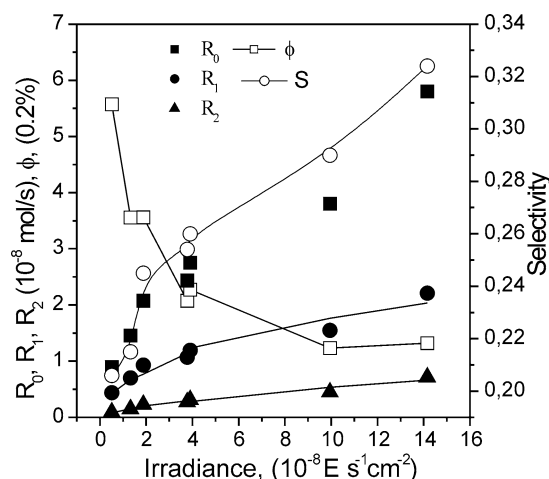


Fig. 2. Influence of irradiance on the rates of ethanol ( $R_1$ ) and acetaldehyde ( $R_2$ ) oxidation, oxygen consumption ( $R_0$ ), selectivity to  $\text{CO}_2$  ( $S$ ), and quantum efficiency ( $\phi$ ). Ethanol concentration 300 ppm, water vapor concentration 4500 ppm, temperature  $40^\circ\text{C}$ , catalyst mass 20 mg.

change only the rate constants of ethanol and acetaldehyde oxidation. The equations for the ethanol and acetaldehyde rates (2) and (3) contain two terms each. Thus, it is impossible to distinguish which item changes more or less in each of the equations when irradiance changes. However, it is possible to estimate which rate constants change more, for ethanol or for acetaldehyde, when irradiance increases. To do this, one needs to assume that the rate constants in both items of Eqs. (2) and (3) follow the same power law. The following equations then determine the irradiance influence:

$$R_1 = \left( R_E^0 + \frac{k_E^0 K_E C_E}{1 + K_E C_E + K_A C_A} \right) \cdot I^\alpha, \quad (4)$$

$$R_2 = \left( \frac{k_A^0 K_A C_A}{1 + K_A C_A} + \frac{k_A^0 K_A C_A}{1 + K_E C_E + K_A C_A} \right) \cdot I^\beta. \quad (5)$$

In Eqs. (4) and (5),  $I$  is irradiance ( $\text{E}/(\text{s cm}^2)$ ),  $\alpha$  and  $\beta$  are exponents dependent on rate constants on irradiance,  $R_E^0$ ,  $k_E^0$ ,  $k_A^0$ , and  $k_A^0$  are the rate and rate constants independent of irradiance, respectively. Eqs. (4) and (5) were fitted to the rates  $R_1$  and  $R_2$  in Fig. 2 using the adsorption constants for ethanol and acetaldehyde determined earlier, and the resultant curves are plotted in Fig. 2. The above assumptions produced relatively good fits to the experimental points with exponents  $\alpha = 0.64$  and  $\beta = 0.46$  for the ethanol and acetaldehyde rate, respectively. Thus, the rate of ethanol photocatalytic oxidation accelerates more than that of acetaldehyde if irradiance increases. This proves the explanation that the increase of selectivity to  $\text{CO}_2$  is associated with the growth of acetaldehyde concentration. If the acetaldehyde concentration were kept constant, the increase of irradiance would result in decrease of the reaction selectivity to  $\text{CO}_2$ . However, Fig. 2 shows a situation that would be preferred in application than keeping a constant acetaldehyde concentration. In air purification, one should increase light intensity in order to obtain higher yields of deep ox-

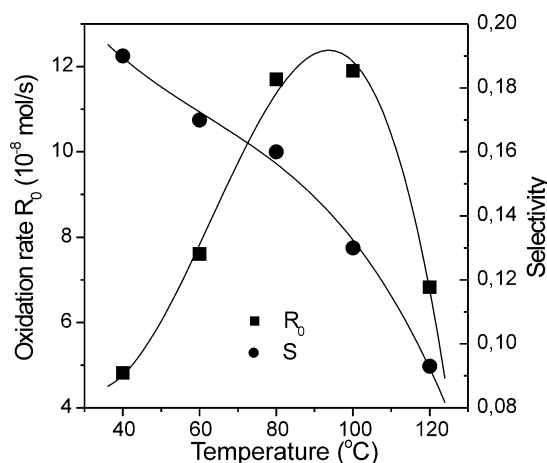


Fig. 3. Effect of temperature on the rate and selectivity of ethanol photocatalytic oxidation over  $\text{TiO}_2$  Hombifine N. Concentration of ethanol adjusted at  $650 \pm 20$  ppm, water concentration 4900 ppm, catalyst mass 26 mg.

idation products if other conditions are kept constant. The decrease of quantum efficiency shown in Fig. 2 will, however, reduce the electric power usage efficiency.

Temperature is one of the factors influencing photocatalytic oxidation that can be easily changed. The influence of temperature on acetone photocatalytic oxidation over  $\text{TiO}_2$  was studied in detail under various conditions previously [15]. The rate of oxidation was highest at temperatures of  $100\text{--}120^\circ\text{C}$  and decreased sharply at higher temperatures. Acetone does not form any significant intermediate gaseous products during photocatalytic oxidation. This is associated with strong adsorption of surface intermediates on the photocatalyst surface. Whereas ethanol forms acetaldehyde and may, therefore, behave differently at increased temperature. Fig. 3 shows how the overall photocatalytic activity expressed as oxygen consumption rate ( $R_0$ ) and selectivity to carbon dioxide change if temperature increases. The data were obtained in the flow-circulating reactor over  $\text{TiO}_2$  Hombifine N photocatalyst. The overall activity increases with temperature until it reaches about  $80^\circ\text{C}$  and decreases at temperatures above  $100^\circ\text{C}$ . No ethanol reaction was detected in dark at any temperature used. This behavior generally resembles that of acetone. However, the thermal deactivation starts at a slightly lower temperature compared to the photocatalytic oxidation of acetone under the same conditions. The concentration of ethanol was kept approximately constant for all points in Fig. 3. Acetaldehyde concentration changed from point to point, starting at 430 ppm at  $40^\circ\text{C}$ , reaching 1341 ppm at  $100^\circ\text{C}$ , and decreasing to 913 ppm at  $120^\circ\text{C}$ . Though the concentration of acetaldehyde increases by almost a factor of 3 as the temperature rises to  $100^\circ\text{C}$ , the selectivity to carbon dioxide decreases monotonically with the increase in temperature, ranging from 0.19 at  $40^\circ\text{C}$  to 0.09 at  $120^\circ\text{C}$ . The decrease in selectivity can be attributed to poisoning  $\text{TiO}_2$  with acetaldehyde at elevated temperatures. Muggli and Falconer [6] used a treatment in acetaldehyde at  $100^\circ\text{C}$  to modify the  $\text{TiO}_2$  surface in order

to increase the selectivity of ethanol photocatalytic oxidation to acetaldehyde. It was suggested that acetaldehyde preferentially deactivates sites with strong ethanol adsorption that are responsible for the deep oxidation of ethanol. In our current study, such TiO<sub>2</sub> surface poisoning can also take place at temperatures around 100 °C. From a practical point of view of air purification, a high concentration of acetaldehyde in the reactor effluent is not desirable and, therefore, photocatalytic treatment of ethanol on TiO<sub>2</sub> should be carried out at lower temperatures.

Loading the TiO<sub>2</sub> surface with platinum was demonstrated to enhance photocatalytic activity for gas-phase reactions in many instances, e.g. [7,14]. For acetone photocatalytic oxidation, the highest rate of reaction was observed on TiO<sub>2</sub> loaded with 0.11 wt% of Pt [14]. Fig. 4 demonstrates how the amount of platinum influences the overall photocatalytic activity in ethanol photocatalytic oxidation carried out in the flow-circulating photocatalytic reactor over platinized TiO<sub>2</sub> Hombifine N. The addition of platinum to TiO<sub>2</sub> results in a marked increase of photocatalytic activity at 40 °C as one can observe by comparing Fig. 4 with the results obtained on pure TiO<sub>2</sub> shown in Figs. 1–3. However, the influence of platinum loading on photocatalytic activity is different from that obtained in acetone photocatalytic oxidation [14]. For acetone oxidation, there was a clear maximum in oxidation rate at loading 0.11 wt% with lower activity at higher and lower loading. For ethanol oxidation, the activity of the sample loaded with 0.1 wt% of Pt was high, the activity of the 0.3 wt% loaded was the lowest, and activity reached a maximum at 1.1 wt% loading. The concentration of acetaldehyde in the reactor changed from 640 for the least active sample, to 800 ppm for the sample with the highest loading. The selectivity to carbon dioxide ranged from 0.23 to 0.26 for different samples of Pt/TiO<sub>2</sub>; i.e., it stayed almost constant. Therefore, the change in acetaldehyde concentration was purely the result of different photocatalytic activity and was a consequence of, not a reason for, different photocatalytic activity.

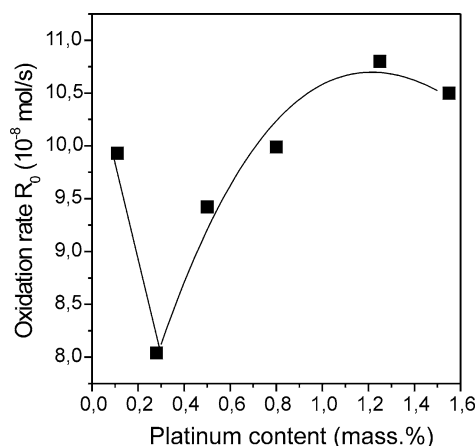


Fig. 4. Rate of ethanol photocatalytic oxidation over TiO<sub>2</sub> with different amounts of deposited platinum. Temperature 40 °C, water concentration 4800 ppm, ethanol concentration adjusted at 300 ppm, catalyst mass 20 mg.

In the previous paper about acetone oxidation on platinum-doped TiO<sub>2</sub>, we observed a significant deviation of platinum content from the target platinum content to lower values [14]. It was connected to removal of platinum particles during photocatalyst washing. In the present study, we used a slightly modified deposition procedure. In order to obtain better contact of platinum with TiO<sub>2</sub> and avoid removal of platinum in washing, vigorous agitation was used during platinum reduction. This modification did result in a better attachment of platinum particles to TiO<sub>2</sub> particles, as the actual platinum content was lower than the theoretical one only for one sample and in that case only by 7%. However, such modification also resulted in a different behavior of platinum-containing photocatalysts as we will see from the results below.

The sample containing 1.1 wt% Pt possessed the highest photocatalytic activity in ethanol photocatalytic oxidation. This sample was chosen for investigation of the influence of temperature on the photocatalytic oxidation of ethanol. Fig. 5 shows the oxygen consumption rate ( $R_0$ ) and selectivity to carbon dioxide in ethanol photocatalytic oxidation at different temperatures in the flow-circulating reactor over this catalyst. Photocatalytic activity over 1.1 wt% Pt/TiO<sub>2</sub> was a maximum at 80 °C. This behavior is similar to that for photocatalytic oxidation over pure TiO<sub>2</sub> (Fig. 3). However, there is 1.5–2 times increase in activity at all temperatures used. The concentration of acetaldehyde also behaves like that in the oxidation over pure TiO<sub>2</sub>—it increases and decreases together with photocatalytic activity. The selectivity of ethanol oxidation to CO<sub>2</sub> over 1.1 wt% Pt/TiO<sub>2</sub> increases with temperature from about 0.14 to 0.20. This observation contrasts with the steady decrease of the selectivity with increase in temperature over pure TiO<sub>2</sub> (Fig. 3). The growth of selectivity to CO<sub>2</sub> is attributable to the thermal catalytic oxidation of acetaldehyde over Pt particles. There was steady-state conversion of acetaldehyde over Pt/TiO<sub>2</sub> at temperatures above 90 °C in dark [16].

The contribution of dark ethanol oxidation over the 1.1% Pt/TiO<sub>2</sub> catalyst is elucidated in Fig. 6. The overall rate of

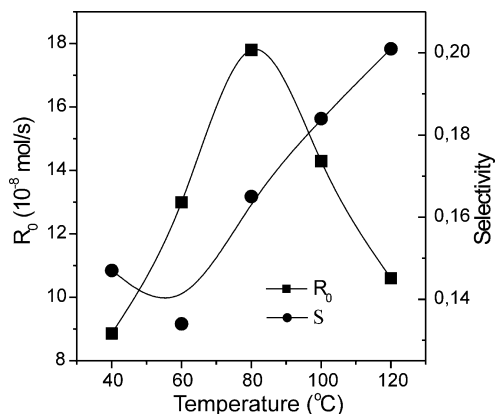


Fig. 5. Rate and selectivity of ethanol photocatalytic oxidation vs temperature over 1.1% Pt/TiO<sub>2</sub> photocatalyst. Ethanol concentration adjusted at 740 ± 90 ppm, water concentration 4900 ppm, catalyst mass 20 mg.

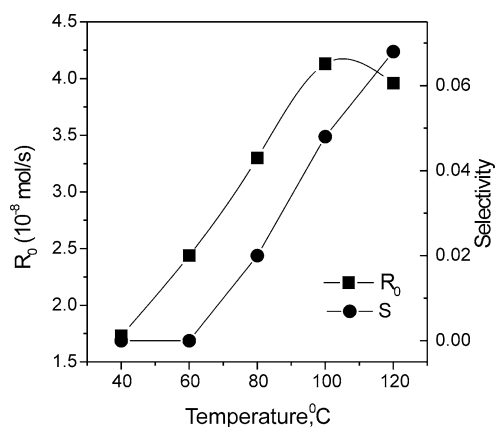


Fig. 6. Rate and selectivity of ethanol oxidation in dark at different temperatures over 1.1% Pt/TiO<sub>2</sub>. Ethanol concentration kept at  $740 \pm 20$  ppm, water concentration 4700 ppm, catalyst mass 20 mg.

oxidation that was performed in the flow-circulating reactor is much smaller compared to the photocatalytic oxidation shown in Fig. 5. At temperatures 40 and 60 °C, only partial oxidation into acetaldehyde is observed, which results in zero selectivity to CO<sub>2</sub>. At higher temperatures, complete oxidation accelerates and selectivity increases. However, neither the growth of overall rate nor the increase in selectivity of ethanol photocatalytic oxidation shown in Fig. 5 can be completely attributed to the effect of thermal oxidation. Its contribution to catalyst performance under irradiation is limited to 20–30%.

In a previous study [14], the photocatalytic activity of platinum-doped titanium dioxide in acetone oxidation steadily increased with increasing temperature. However, in the present study, the photocatalytic activity in ethanol oxidation has a peak. The different temperature dependencies could be associated with either the different substrate or the different properties of the photocatalyst. In order to check the influence of organic substrate, acetone was tested over the same photocatalyst as used for ethanol oxidation. Fig. 7 shows the influence of temperature on acetone pho-

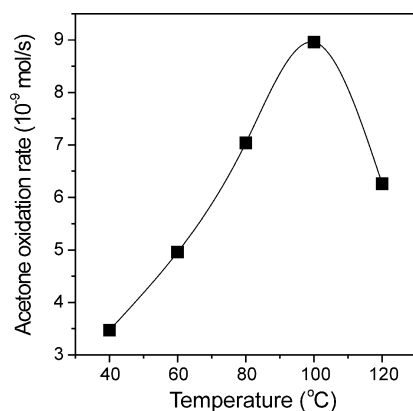


Fig. 7. Effect of temperature on the rate of acetone photocatalytic oxidation over 1.1% Pt/TiO<sub>2</sub> photocatalyst. Acetone concentration 600 ppm, water concentration 5000 ppm, catalyst mass 20 mg.

tocatalytic oxidation over the sample containing 1.1% Pt on Hombifine N, which was measured in the flow-circulating reactor. There is a clear peak in the oxidation rate at 100 °C. Since the peak in temperature dependence was observed for both acetone and ethanol, it is not associated with a specific organic compound but should be related to properties of the photocatalyst. As we pointed out above, the Pt/TiO<sub>2</sub> photocatalyst used in this study possesses intimate contact between the particles of titania and platinum. Such close contact causes a decrease in the photocatalytic activity at temperatures above 100 °C. This was comprehensively proved by Kennedy and Datye [13], who compared several photocatalysts. The first was TiO<sub>2</sub> loaded with platinum using photodeposition, and the second was a physical mixture of TiO<sub>2</sub> and Pt/SiO<sub>2</sub>. TEM showed good contact of Pt with TiO<sub>2</sub> in the first photocatalyst and the second one obviously did not possess close interaction of TiO<sub>2</sub> and Pt. The first photocatalyst showed a decrease in CO<sub>2</sub> production rate above 100 °C, while the activity of the second photocatalyst steadily increased with temperature.

Loading titania with platinum significantly enhances its photocatalytic activity and can change the product distribution. Studies on products are carried out most conveniently in batch reactors [2]. We used a small glass batch reactor for testing the pure and platinum-doped homemade TiO<sub>2</sub> in the photocatalytic oxidation of ethanol. Fig. 8a shows profiles of concentration during oxidation over TiO<sub>2</sub>. The starting ethanol concentration was about 920 ppm, which corresponds to 17  $\mu$ mol of ethanol in the gas phase and 17  $\mu$ mol adsorbed on the TiO<sub>2</sub> surface. Acetaldehyde was the main gaseous intermediate and reached a maximum concentration of 770 ppm after 80 min of reaction. The formation of a significant amount of carbon monoxide was also noted. Its concentration reached 80 ppm at a reaction time of 164 min. Carbon dioxide was the final product, with a final concentration (164 min) of about 1620 ppm. The concentration of carbon monoxide did not seem to decrease during this run. Pure TiO<sub>2</sub> has a very low activity for the CO oxidation. The quantum yield for CO oxidation was reported to be only about 2% whereas the quantum yield for acetone oxidation was 40–60% [4].

Ethanol photocatalytic oxidation over platinum-doped TiO<sub>2</sub> demonstrated different concentration profiles (Fig. 8b). The starting ethanol concentration was 1230 ppm, which corresponds to 23  $\mu$ mol of ethanol in the gas phase and 11  $\mu$ mol in the adsorbed state on TiO<sub>2</sub>. Platinum-doped TiO<sub>2</sub> adsorbed significantly less ethanol than the unplatinated one. The profile of acetaldehyde concentration had a maximum of about 810 ppm at 70 min. By the end of the experiment (160 min), the acetaldehyde concentration had fallen to almost zero. The maximum acetaldehyde concentration was about the same over platinum-containing and nonplatinum-containing TiO<sub>2</sub>, but acetaldehyde concentration decreased much more slowly over TiO<sub>2</sub> and had not approached zero at the end of observation. Carbon monoxide was not detected

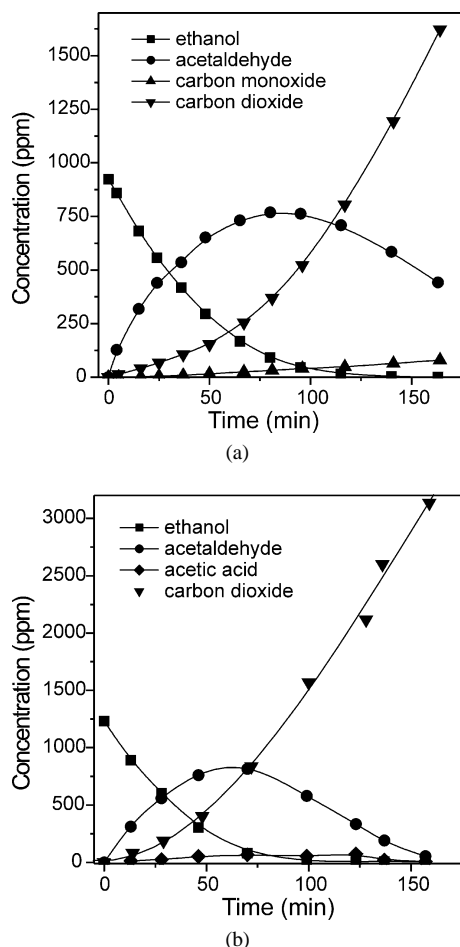


Fig. 8. Photocatalytic oxidation of 2  $\mu\text{l}$  of ethanol in a batch reactor at 25 °C: (a) over 20 mg of  $\text{TiO}_2$ , (b) over 20 mg of 0.5% Pt/ $\text{TiO}_2$ .

in ethanol photooxidation over Pt/ $\text{TiO}_2$ . This is explained by the high photocatalytic activity of platinum-doped titanium dioxide in CO oxidation. In a previous study, the quantum yield of CO oxidation over Pt/ $\text{TiO}_2$  was 37%, which is much larger than that over  $\text{TiO}_2$  [4]. Instead of CO, acetic acid was detected in the products over Pt/ $\text{TiO}_2$ . Its concentration reached a maximum of about 70 ppm at 123 min and decreased to 8 ppm by the end of the experiment. A significant amount of acetic acid in the gas phase may be associated with a reduced adsorption capacity of the photocatalyst. An increased starting concentration of ethanol over Pt/ $\text{TiO}_2$  with the same total amount of ethanol in the reactor corroborates this. The generation of carbon dioxide was significantly faster over platinum-doped  $\text{TiO}_2$ . The  $\text{CO}_2$  concentration reached 3140 ppm at the end of observation, which was about twice that of pure  $\text{TiO}_2$  under the same conditions. Thus, the application of platinum-doped titanium dioxide for ethanol photocatalytic oxidation avoided carbon monoxide in the gaseous products and resulted in twice the rate of deep oxidation. These are definitely beneficial effects from a practical point of view.

#### 4. Conclusions

The rates of the two main steps in ethanol photocatalytic oxidation were studied at different concentrations of ethanol and acetaldehyde and were demonstrated to follow the semi-empirical Langmuir–Hinshelwood model with three types of adsorption site—those available for ethanol only, those available for acetaldehyde only, and those available for both molecules. An increase in acetaldehyde concentration improved selectivity toward complete oxidation.

An increase of  $\text{TiO}_2$  photocatalyst irradiance improved the selectivity to  $\text{CO}_2$  via the increase in acetaldehyde concentration. However, the rate constant of ethanol oxidation increased faster than that of acetaldehyde and the quantum efficiency decreased at higher irradiance.

If the reactor temperature increased to 80 °C the overall reaction rate over  $\text{TiO}_2$  increases but a decrease occurs at higher temperatures. The selectivity to  $\text{CO}_2$  decreases monotonically as temperature is increased.

The addition of platinum to  $\text{TiO}_2$  leads to optimum performance at a platinum content of 1.1 wt%. The overall reaction rate increases 1.5- to 2-fold at all temperatures used and the selectivity to  $\text{CO}_2$  monotonically rises with temperature.

Platinum addition also resulted in a change of minor reaction products. Carbon monoxide was not observed over platinum-containing catalysts but the concentration of acetic acid was increased.

#### Acknowledgments

The support of INTAS via fellowship YSF 2002-55 is gratefully acknowledged. We acknowledge the support of RFBR through Grant 02-03-08002.

#### References

- [1] M.L. Sauer, D.F. Ollis, *J. Catal.* 158 (1996) 570.
- [2] M.R. Nimlos, E.J. Wolfrum, M.L. Brewer, J.A. Fennell, G. Bintner, *Environ. Sci. Technol.* 30 (1996) 3102.
- [3] D.S. Muggli, S.A. Larson, J.L. Falconer, *J. Phys. Chem.* 100 (1996) 15886.
- [4] A.V. Vorontsov, E.N. Savinov, G.B. Barannik, V.N. Troitsky, V.N. Parmon, *Catal. Today* 39 (1997) 207.
- [5] D.S. Muggli, J.T. McCue, J.L. Falconer, *J. Catal.* 173 (1998) 470.
- [6] D.S. Muggli, J.L. Falconer, *J. Catal.* 175 (1998) 213.
- [7] J.C. Kennedy, A.K. Datye, *J. Catal.* 179 (1998) 375.
- [8] D.S. Muggli, K.H. Lowery, J.L. Falconer, *J. Catal.* 180 (1998) 111.
- [9] S.-J. Hwang, D. Raftery, *Catal. Today* 49 (1999) 353.
- [10] S. Pilkenton, S.-J. Hwang, D. Raftery, *J. Phys. Chem. B* 103 (1999) 11152.
- [11] D.V. Kozlov, E.A. Paukshtis, E.N. Savinov, *Appl. Catal. B* 24 (2000) L7.
- [12] A.V. Vorontsov, E.N. Savinov, *Chem. Eng. J.* 70 (1998) 231.
- [13] J.C. Kennedy, A.K. Datye, *J. Catal.* 179 (1998) 375.
- [14] A.V. Vorontsov, I.V. Stoyanova, D.V. Kozlov, V.I. Simagina, E.N. Savinov, *J. Catal.* 189 (2000) 360.
- [15] A.V. Vorontsov, E.N. Kurkin, E.N. Savinov, *J. Catal.* 186 (1999) 318.
- [16] J.L. Falconer, K.A. Magrini-Bair, *J. Catal.* 179 (1998) 171.